

# DYNAMIC FRICTIONAL BEHAVIOUR OF SYNTHETIC SANDSTONE UNDER LOW NORMAL STRESS AND SEISMIC EXCITATION

Kuo Chen Lee<sup>1</sup>, Rolando P. Orense<sup>2</sup> and Fu Shu Jeng<sup>3</sup>

## SUMMARY

Both New Zealand and Taiwan are located in the Pacific ring of fire, the most active seismic zone in the world, and therefore slope failures triggered by seismic excitation are frequent and they sometimes could cost severe damage to life and property. Earthquake induced slope failure, especially rock-block sliding failure, is usually analysed using friction coefficient measured at the sliding-interface. A tilt test is a convenient test for measuring the required values under static condition, but the applicability of measured results to analyse block sliding under dynamic condition requires further investigation. In this paper, a series of static tilt test and dynamic shaking table test were performed to simulate block sliding with base excitation. The results were compared in terms of measured sliding thresholds, and the causes of the differences were discussed. Tests on synthetic sandstone showed that friction coefficients measured by tilt tests were always larger than the ones derived by shaking table tests. Furthermore, sliding thresholds increased with increasing shaking frequency, suggesting that the sliding threshold is non-constant under excitation. In addition, the sliding threshold is lower at higher contact stresses on the sliding surface, showing that the sliding threshold varies with normal stress. This study identified the limitations of the tilt test when applied to dynamic problems, and recommended that realistic sliding threshold can only be obtained using dynamic tests, such as shaking table tests.

## INTRODUCTION

On September 21 in 1999, a severe earthquake with  $M_L$  7.3 shocked central Taiwan. More than 2,400 people were killed in this event, and many properties all over the country were damaged enormously. Some large scale rockslides were triggered by the quake, more popularly referred to as the Chi-Chi earthquake. One of the most damaging types is the deep-seated slope-failures, such as those observed in Tsaoling and Jiufengershan, which caused massive damages and casualties (Kamai *et al.*, 2000; Huang *et al.*, 2002).

The effects of earthquakes on rockslides are often analysed using pseudo-static method (Terzaghi, 1950) or a block-sliding method (Newmark, 1965; Jibson and Keefer, 1993; Wartman *et al.*, 2000; Kokusho and Ishizawa, 2007; Chiang *et al.*, 2009). Both methods make use of friction coefficient at the sliding-interface to study the sliding process. In general, the friction coefficient is related to the surface structure (i.e. grain size of parent rock) with asperities and interlocking playing an important role.

In analysing rigid block movement at an interface, the Coulomb's friction law has been traditionally used, The static friction coefficient between the block and the sliding surface is defined as the ratio of the tangential force required to produce sliding divided by the normal force between the surfaces. When the tangential force overcomes the frictional force between the two surfaces, then the block starts to move. The sliding frictional resistance is normally different to the static frictional resistance. The coefficient of sliding (or kinetic)

friction, is expressed using the same formula as the static coefficient but is generally lower in value.

For slope stability analyses considering only gravity effect, i.e. static loading condition or no base excitation, a tilt test is a convenient and reasonable test method for measuring friction coefficient (Barton and Choubey, 1977). However, the friction angle obtained from a tilt test is questionable when applied to the analysis of dynamic problems. For example, its applicability in Newmark analysis to determine the sliding threshold requires further investigation.

This study was intended to identify quantitatively the difference between measured sliding thresholds for a block on a slope subjected to base excitation through laboratory experiments. Note that it is often found that friction coefficients obtained using back-analyses on large-scale earthquake-induced rockslides with deep-seated failure surface tend to be smaller than the ones obtained using laboratory tests, such as in direct shear test, cyclic shear test and tilt test (Hencher, 1980; Barbero *et al.* 1996; Shou and Wang, 2003; Jafari *et al.* 2004). The difference in the scale (large- versus small-scale) and in the loading conditions (dynamic versus static loading) also play a role in the discrepancy between back-calculated and laboratory-measured friction angles. Finally, the applicability of a tilt test-derived friction coefficient in determining the sliding threshold of earthquake-induced landslides is discussed by comparing the sliding thresholds obtained with those from small-scale shaking table tests at similar levels of normal stresses, thereby eliminating the scale effect.

<sup>1</sup> Senior Engineer, CECI Engineering Consultants Inc., Taiwan (formerly PhD Student, National Taiwan University, Taiwan).

<sup>2</sup> Senior Lecturer, Department of Civil and Environmental Engineering, University of Auckland, Auckland, New Zealand.

<sup>3</sup> Professor, Department of Civil Engineering, National Taiwan University, Taipei, Taiwan.

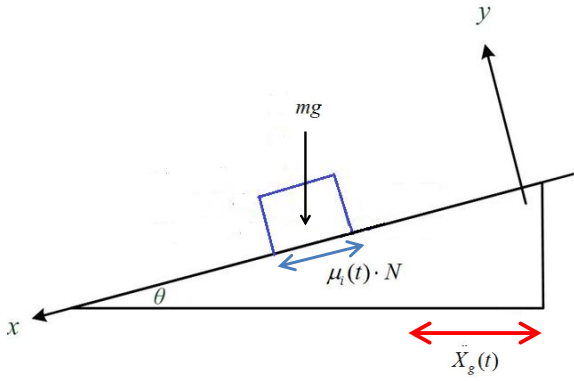


Figure 1: Illustration of the force equilibrium for a sliding block on a slope.

### RESPONSE OF SLIDING RIGID BLOCK

Figure 1 illustrates a rigid block sliding down an inclined plane under the action of a horizontal acceleration. In the figure,  $m$  is the mass of the sliding block,  $g$  is the gravitational acceleration,  $\theta$  is the slope angle,  $N$  the component of the reaction force of the slope on the block,  $\mu_i(t)$  is the instantaneous friction coefficient and  $\ddot{X}_g(t)$  is the temporal acceleration at base. Considering force equilibrium in the  $y$ -direction:

$$N = mg \cos \theta + m \left| \ddot{X}_g(t) \right| \sin \theta \operatorname{sgn}(\ddot{X}_g(t)) \quad (1)$$

where  $\operatorname{sgn}$  is the signum function. Re-arranging this equation:

$$\frac{N}{m \cos \theta} = g + \left| \ddot{X}_g(t) \right| \tan \theta \operatorname{sgn}(\ddot{X}_g(t)) \quad (2)$$

The force equilibrium in the  $x$  direction can be written in terms of the instantaneous friction coefficient,  $\mu_i(t)$ , as follows:

$$mg \sin \theta - m \left| \ddot{X}_g(t) \right| \cos \theta - \mu_i(t) N \operatorname{sgn}(\ddot{X}_r(t)) = m \ddot{X}_r(t) \quad (3)$$

where  $\ddot{X}_r(t)$  is the relative acceleration between the block and the plane which has no component along the  $y$ -axis. Re-arranging Equation (3):

$$\mu_i(t) = \frac{-\left| \ddot{X}_g(t) \right| \cos \theta - \left| \ddot{X}_r(t) \right| + g \sin \theta}{\frac{N}{m} \operatorname{sgn}(\ddot{X}_r(t))} \quad (4)$$

When the block starts to slide, the friction coefficient is defined by instantaneous critical friction coefficient,  $\mu_c = \mu_i(t_c)$ , which is the measured instantaneous friction coefficient at the initiation of sliding, i.e.  $t = t_c$ .

$$mg \sin \theta - m \left| \ddot{X}_g(t) \right| \cos \theta = \mu_c N \operatorname{sgn}(\ddot{X}_r(t)) \quad (5)$$

Figure 2 illustrates some of the important parameters used in this study. Instantaneous friction coefficient,  $\mu_i(t)$ , is the mobilised friction coefficient and hence is an indicator of the stress state at the interface. This is the friction coefficient derived from shaking table tests and is different from  $\mu_t$  measured using tilt tests, which was proposed by Mendez *et al.* (2009) and Chaudhuri and Hutchinson (2005). Note that  $\mu_t$  and  $\mu_c$  are sliding thresholds and hence defines the strength of the interface. The critical acceleration,  $A_c$ , defined by Newmark (1965), is the acceleration measured at  $t = t_c$ . These quantities are derived in this study from measurements using the shaking table. Finally,  $\mu_{i, \max}$  is the maximum value measured in one cycle.

### LABORATORY TESTS

In this work, two types of experiments were conducted: tilt test and small-scale shaking table test. The results were compared to investigate the applicability of the frictional parameters obtained using a tilt test in analysing earthquake-induced rock block slide.

#### Tilt test

Barton and Choubey (1977) proposed a tilt test to measure the maximum static friction angle  $\phi_t$  at the sliding interface under low normal stress condition. The present paper follows the same procedure to obtain these parameters for comparison with those obtained from shaking table tests. The experimental set-up is illustrated in Figure 3(a). Note that the friction coefficient  $\mu_t$  derived from the maximum static friction angle  $\phi_t$  is considered as the sliding threshold obtained using tilt tests.

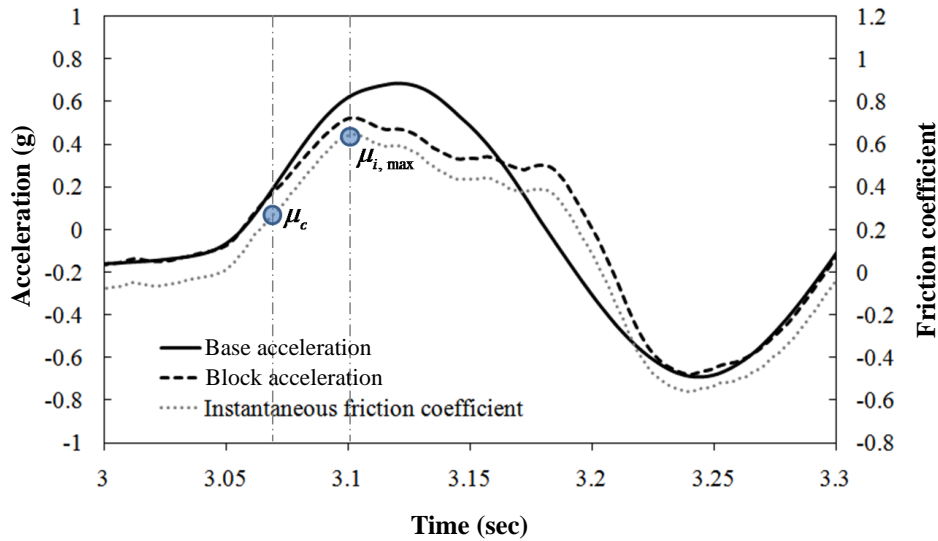
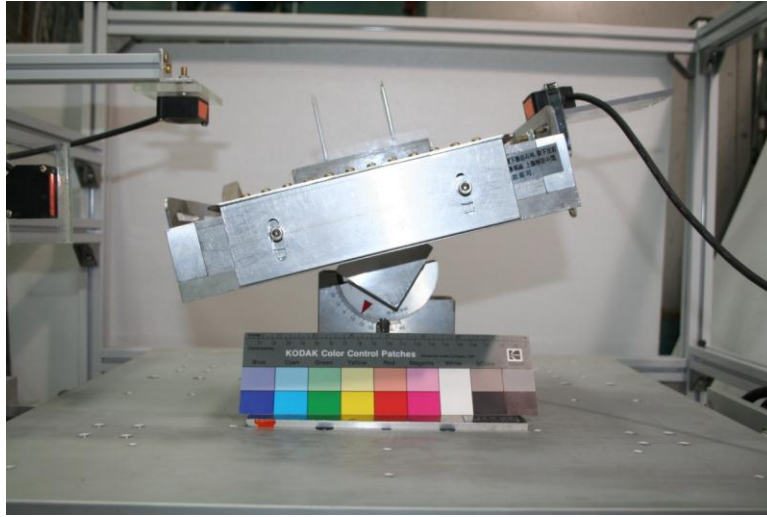
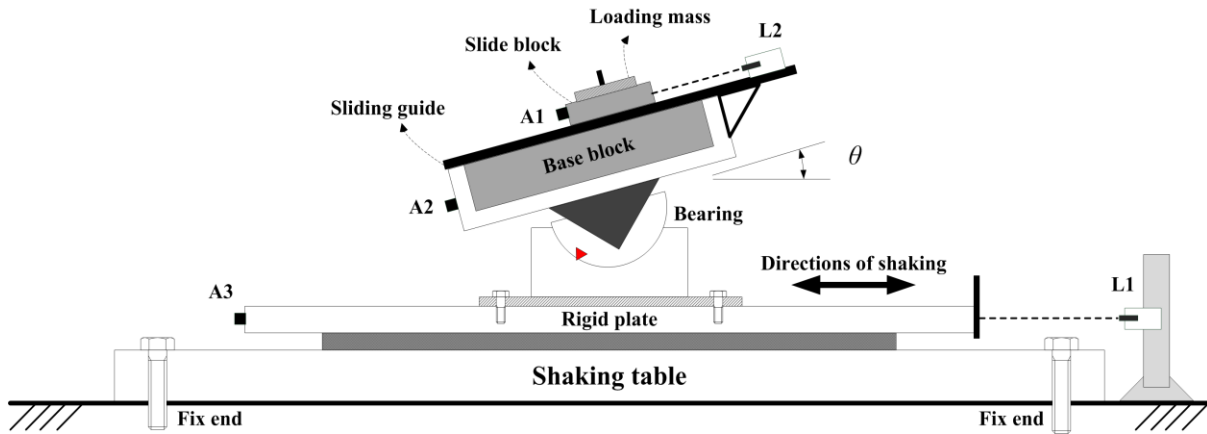


Figure 2: Definition of important parameters used in this study.



(a) Tilt table test



(b) Shaking table test

Figure 3: Experimental set-up for the tests.

### Shaking table test

The setup of shaking table test, shown in Figure 3(b), follows related works (Wartman *et al.*, 2003; Park *et al.*, 2006; Mendez *et al.* 2009) where sliding between a block and the base was induced using the shaking table. The shaking table used in the study has the following features: (a) controlled excitation through a servo-control system with fixed frequency of sine wave; (b) the bearing allows a free adjustment to the slope angle; and (c) the sliding guide ensures the sliding block moves one-dimensionally on the base block.

Auxiliary uniaxial accelerometers (PCB-3711D1FA3G) at A1, A2 and A3 locations recorded the temporal accelerations of the sliding block, the base block, and the rigid plate driven by the servo-control system, respectively. High precision laser displacement sensors (Keyence LK-G155) with accuracy of 0.01 mm were installed at L1 and L2 positions to measure the temporal displacement of the base and the sliding block, respectively. Rather than using the relative acceleration between the sliding block and the base block (A2-A1) to define the initiation time of sliding,  $t_c$ , this paper proposed the use of direct measurement of relative displacement by L2 to obtain  $t_c$ . From the laboratory tests conducted by the authors, the proposed method identifies  $t_c$  more accurately than the former method when the relative displacement between the sliding

block and base is small. Furthermore, it should be mentioned that the accelerations of the base and of the sliding block were also checked from these displacement measurements (by taking time derivatives twice). The friction coefficients derived at  $t_c$  were then used as the sliding thresholds.

## TEST RESULTS

### Comparison of Sliding Thresholds

The differences between  $\mu_c$  and  $\mu_t$  were investigated by conducting both tilt test and shaking table test on three selected block and base materials: aluminium, MS4 sandstone and synthetic sandstone. Descriptions of the two sandstones were provided by Jeng *et al.* (2004) and by Jafari *et al.* (2004), respectively.

Tilt tests were performed using the set-up discussed earlier, and the results over several trials are shown in Figure 4. The error bar in the figure denotes the range of maximum and minimum values obtained in the trials. Similarly, the same specimens were then tested using the shaking table to measure  $\mu_c$ . The shaking table test results performed with slope inclination  $\theta = 0^\circ$ , excitation frequency,  $f = 4$  Hz and peak ground acceleration,  $PGA = 0.7g$  are also plotted in Figure 4, where the mean and the range of values are indicated. From

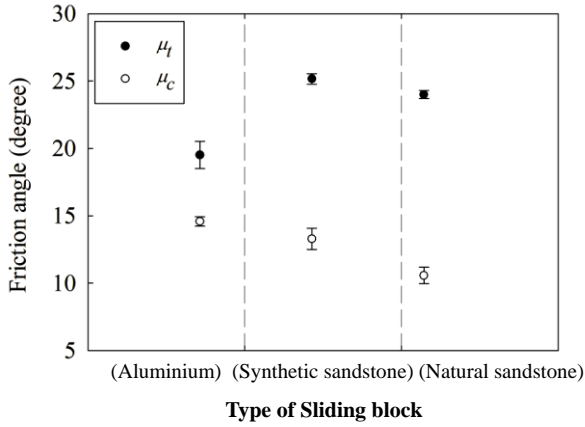


**Figure 4:** Comparison of friction coefficients  $\mu_t$  from tilt test and  $\mu_c$  from shaking table test with different types of sliding blocks. Shaking table tests were at  $\theta = 0^\circ$ ,  $f = 4$  Hz and  $PGA = 0.7g$ . The error bar denotes the range of values obtained from several trials.

comparison of the test results, it is seen that the measured  $\mu_c$  is consistently less than  $\mu_t$  for all types of surfaces considered. Furthermore, sandstone and synthetic sandstone show the largest deviation between the two coefficients with reduction in value close to 50%. These results suggest that the sliding threshold can be reduced by the presence of base excitation.

Under different shaking frequencies, the coefficients  $\mu_c$  and  $\mu_{i,max}$  show different tendencies, as shown in Figure 5. Also indicated in the figure are the frictional coefficients derived from tilt test,  $\mu_t$ , as well as the kinetic friction,  $\mu_k$ . The instantaneous critical friction coefficient  $\mu_c$  increases as the shaking frequency increases. On the contrary, the maximum friction coefficient at each cycle,  $\mu_{i,max}$ , decreases with higher shaking frequency. At the highest shaking frequency of 8 Hz, the two friction coefficients appear to converge.

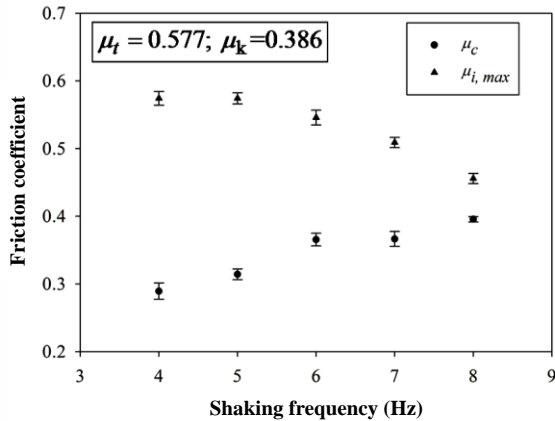


**Figure 5:** Comparison between  $\mu_c$  and  $\mu_{i,max}$  measured from shaking table test under different shaking frequencies ( $\theta = 0^\circ$  and  $PGA = 0.7g$ ). The error bar denotes the range of values obtained from several trials.

#### Influence of applied normal force and shaking frequencies

Next, the effects of excitation frequencies and applied normal stresses on the friction coefficients  $\mu_c$  and  $\mu_{i,max}$  were investigated using a shaking table. Emphasis was placed on how the excitation frequency and the applied normal stress

**Table 1:** Static friction coefficients of synthetic sandstone under different normal stresses

Different applied normal stresses	Normal stress (kPa)	$\mu_t$
$(\sigma_n)_{A1}$	0.635	0.577
$(\sigma_n)_{A2}$	0.781	0.573
$(\sigma_n)_{A3}$	1.38	0.575
$(\sigma_n)_{A4}$	3.31	0.569
$(\sigma_n)_{A5}$	5.93	0.577

affect the sliding threshold. For this purpose, a series of tests were conducted using synthetic sandstone. The changes in the magnitude of  $\mu_c$  was investigated under three different slope angles ( $0^\circ$ ,  $5^\circ$  and  $10^\circ$ ), five different shaking frequencies (ranging from  $f = 4 - 8$  Hz) and five levels of applied normal stress. The magnitudes of these initial normal stresses, which were varied by adding mass on top of the sliding block, are listed in Table 1, together with the corresponding  $\mu_t$ . Note that in performing the tests, we had to make sure that the toppling of the sliding block will not occur during the sliding process.

Figure 6 shows the comparison of  $\mu_c$  values for different inclination angles,  $\theta$ , at shaking frequencies of 4 and 6 Hz. Regardless of the value of  $\theta$ , the magnitude of  $\mu_c$  appears to be related to the excitation frequency. The value increases with excitation frequency, although the difference becomes negligible at steeper inclination angle.

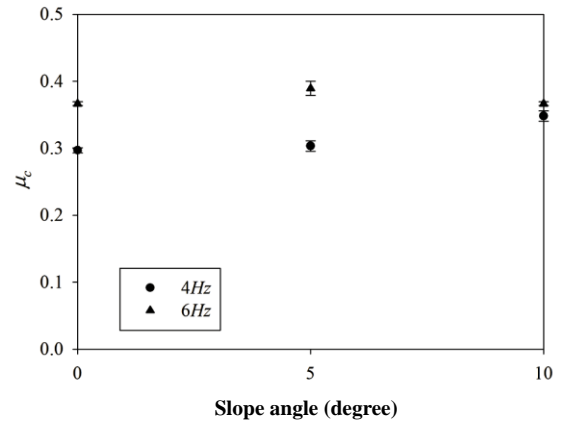


**Figure 6:** Effect of slope inclination on the measured  $\mu_c$  at different excitation frequencies using synthetic sandstone ( $PGA = 0.7g$ ). The error bar denotes the range of values obtained from several trials.

On the other hand, Figure 7 shows the variation of  $\mu_c$  with shaking frequency for different applied initial normal stresses. It is seen that higher excitation frequency results in higher sliding threshold coefficient. From the test results, an increase of 1 Hz in excitation frequency causes an increase in  $\mu_c$  by 5.2 – 12.6%. In addition, it is noted that with each increase in normal stress by 100%, the value of  $\mu_c$  decreases by about 20%.

Figure 8 plots the values of  $\mu_{i,max}$  for different shaking frequencies and applied initial normal stresses. It is clear that  $\mu_{i,max}$  decreases with increasing normal stress and increasing excitation frequency, such as that observed at 7 – 8 Hz range.

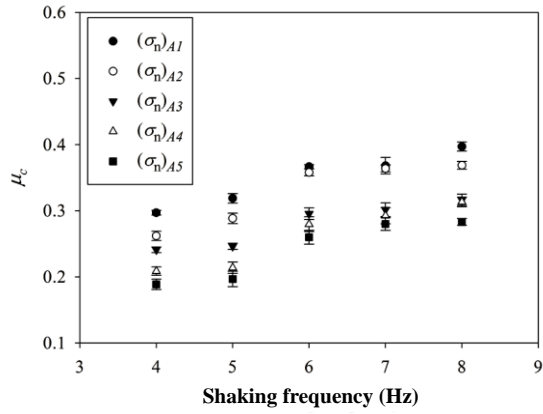


**Figure 7:** Effect of shaking frequency on the measured  $\mu_c$  under different applied initial normal stresses ( $\theta = 5^\circ$  and  $\text{PGA} = 0.7g$ ). The error bar denotes the range of values obtained from several trials.

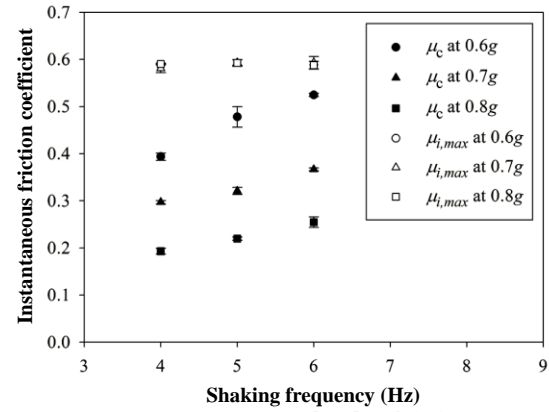


**Figure 9:** Effect of shaking frequency on the measured  $\mu_c$  and  $\mu_{i,max}$  under different peak acceleration amplitudes (Synthetic sandstone and  $\theta = 5^\circ$ ). The error bar denotes the range of values obtained from several trials.

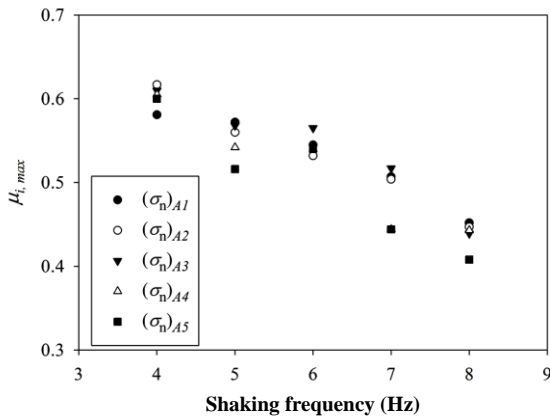


**Figure 8:** Effect of shaking frequency on the measured  $\mu_{i,max}$  under different applied initial normal stresses ( $\theta = 5^\circ$  and  $\text{PGA} = 0.7g$ ). The error bar denotes the range of values obtained from several trials.

### Influence of Peak Acceleration Amplitudes

Finally, the effects of the peak amplitude of the input base acceleration on the threshold values were investigated. For this purpose, three different peak acceleration amplitudes, i.e., 0.6g, 0.7g and 0.8g, were employed in the shaking table tests to study their effects on  $\mu_c$  and  $\mu_{i,max}$ . The shaking frequencies were varied from 4 – 6 Hz. The test results are summarised in Figure 9, where it is seen that increasing peak acceleration amplitudes decreases  $\mu_c$  regardless of the excitation frequency. With each increase in peak acceleration amplitudes by 0.1g,  $\mu_c$  decreases by roughly 25%. On the other hand, the test results indicate that  $\mu_{i,max}$  is not affected by the different peak acceleration amplitudes, at least within the range of values considered in the tests.

### SUPPLEMENTARY ANALYSIS

The shaking table test results clearly illustrated the difference between the thresholds obtained for sliding when compared to those obtained using tilt test. Two factors need to be explained further: (1) the influence of additional inertia forces induced by excitation; and (2) the influence of the roughness of the sliding surface.

Regarding the effect of additional inertia forces, the experimental results presented herein consistently showed that the measured  $\mu_c$  from shaking table tests are significantly smaller than  $\mu_t$  measured in tilt tests. This suggests that, under the same static normal stress, the additional inertia forces induced by the excitation at base could be a key factor in causing  $\mu_c < \mu_t$ . Moreover, the additional inertial force induced by the excitation increases with increase in peak acceleration amplitude and increase in shaking frequency. It is inferred that the additional inertia forces change the uniformity of stress distribution under the sliding block during sliding, resulting in a reduction of  $\mu_c$  as compared to  $\mu_t$ .

Next, the influence of the roughness on the sliding surface needs to be further discussed. Figure 10 is the top view of the surface of the synthetic sandstone observed from an optical electron microscope. The synthetic sandstone is composed of cement, quartz sand and water (at a ratio of 1 : 2.5 : 0.75), and therefore, the conceptual contact model of the sliding block can be imagined to that illustrated in Figure 11. At the rock interface, the resistance is mobilised at the beginning of shearing. When the block's initial relative sliding is triggered by excitation, the friction coefficient is the sliding threshold of block,  $\mu_c$ . After the block's initial relative sliding, the friction coefficient becomes  $\mu_t(t)$ . At the instant the asperities are sheared,  $\mu_t(t)$  reaches its maximum value,  $\mu_{i,max}$ . In some cases, the asperities climb over one another, resulting in higher friction resistance, and this is manifested with values of  $\mu_{i,max}$  being greater than that of  $\mu_c$ . The frictional resistance



**Figure 10:** View of the surface of synthetic sandstone through an optical electron microscope.

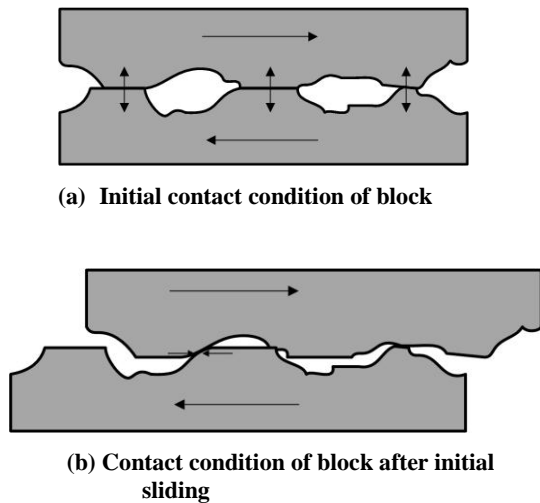


Figure 11: A conceptual contact model for synthetic sandstone.

decreases because of the mechanical degradation. Moreover, when the applied confining pressure is high, some asperities are flattened, resulting in a general decrease in resistance.

### CONCLUDING REMARKS

In this study, the applicability of a tilt test-measured sliding threshold,  $\mu_t$ , in dynamic analyses was clarified. Using  $\mu_t$  in sliding block analyses under base excitation would lead to underestimating the cumulative relative displacement due to the overestimated frictional resistance. Therefore, the sliding threshold should be defined using dynamic tests, such as the shaking table tests used in this study.

The authors plan to continue studying how normal stresses of different scales could be used in analysing sliding blocks, and to research the effect of excitation characteristics (such as duration of shaking and influence of the vertical base excitation) on the sliding threshold and frictional behaviours during sliding.

Moreover, based on experiments performed using aluminium, sandstone, and synthetic sandstone, it has been shown that the type of material strongly dictates the observed frictional behaviour on both sliding threshold and instantaneous friction coefficient during sliding. Therefore, in order to establish rock block or rock slope sliding models during excitation, it is necessary to use frictional model based on measured behaviour on real rock materials or synthetic rock materials. We plan to continue experiments on real rock specimens (e.g. sandstone, shale, siltstone, etc.) to build up representative mechanical models for rocks during sliding under excitation, which can be applied to analyses of real cases.

### ACKNOWLEDGMENTS

The authors wish to express their appreciation to the National Science Council (NSC), Taiwan for the financial support provided under Project No. NSC 97-2221-E-002-187. Thanks are also due to the Department of Civil and Environmental Engineering, University of Auckland for making this research possible.

### REFERENCES

Barbero, M., Barla, G. and Zaninetti, A. (1996). "Dynamic shear strength of rock joints subjected to impulse loading," *International Journal of Rock Mechanics & Mining Sciences*, **33** (2), 141-151.

- Barton, N. and Choubey, V. (1977). "The shear strength of rock joints in theory and practice," *Rock Mechanics*, **10**, 1-54.
- Chaudhuri, S.R. and Hutchinson, T.C. (2005). "Characterizing frictional behavior for use in predicting the seismic response of unattached equipment," *Soil Dynamics and Earthquake Engineering*, **25**, 591-604.
- Chiang, T.L., Wang T.T., Lee, K.C. and Jeng, F.S. (2009). "Analysis of pyramidal block slide induced by seismic excitation," *Journal of the Chinese Institute of Engineers* **32** (1), 107-122.
- Hencher, S. R. (1980). "Friction parameters for the design of rock slopes to withstand earthquake loading," *Design of Dams to Resist Earthquake*, ICE, London.
- Huang, C.S., Chen, M.M. and Hsu, M.I. (2002). "A preliminary report on the Chiufenershan landslide triggered by the 921 Chi-Chi earthquake in Nantou, central Taiwan," *Terrestrial, Atmospheric and Oceanic Sciences* **13**, 387-395.
- Jafari, M.K., Pellet, F., Boulonb, M. and Amini Hosseini, K. (2004). "Experimental study of mechanical behavior of rock joints under cyclic loading," *Rock Mechanics and Rock Engineering*, **37** (1), 3-23.
- Jeng, F.S., Weng, M.C., Lin, M.L. and Huang, T.H. (2004). "Influence of petrographic parameters on geotechnical properties of tertiary sandstones from Taiwan," *Engineering Geology* **73**, 71-91.
- Jibson, R.W. and Keefer, D.K. (1993). "Analysis of the seismic origin of landslides: Examples from New Madrid seismic zone," *Geological Society of America Bulletin*, **105**, 521-536.
- Kamai, T., Wang, W.N. and Shuzui, H. (2000). "The landslide disaster induced by the Taiwan Chi-Chi earthquake of 21 September 1999," *Landslide News*, **13**, 8-12.
- Kokusho, T. and Ishizawa, T. (2007). "Energy approach to earthquake-induced slope failures and its implications," *Journal of Geotechnical and Geoenvironmental Engineering*, **133** (7), 828-840.
- Mendez, B.C., Botero, E. and Romo, M.P. (2009). "A new friction law for sliding rigid blocks under cyclic loading," *Soil Dynamics and Earthquake Engineering*, **29**, 874-882.
- Newmark, N.M. (1965). "Effect of earthquakes on dams and embankments," *Geotechnique*, **15** (2), 139-160.
- Park, B.K., Jeon, S. and Lee, C.S. (2006). "Evaluation of dynamic frictional behavior of rock joints through shaking table test," *Tunnelling and Underground Space Technology*, **21**, 427.
- Shou, K.J. and Wang, C.F. (2003). "Analysis of the Chiufengershan landslide triggered by the 1999 Chi-Chi earthquake in Taiwan," *Engineering Geology*, **68**, 237-250.
- Terzaghi, K. (1950). "Mechanisms of landslides, In Application of Geology to Engineering Practice (Berkeley Volume)," edited by S. Paige, *Geological Society of America*, New York, 83-123.
- Wartman, J., Riemer, M.F., Bray, J.D. and Seed, R.B. (2000). "Newmark analysis of a shaking table slope stability experiment," *Geotechnical Earthquake Engineering and Soil Dynamics*, **3**, 778-789.
- Wartman, J., Bray, J. D. and Seed, R.B. (2003). "Inclined plane studies of the Newmark sliding block procedure," *Journal of Geotechnical and Geoenvironmental Engineering*, **129** (8), 673-684.